

Regular article

Computational and qualitative aspects of evolution of curves driven by curvature and external force*

Karol Mikula¹, Daniel Ševčovič²

¹ Department of Mathematics, Slovak University of Technology, Radlinského 11, 813 68 Bratislava, Slovak Republic
(e-mail: mikula@vox.svf.stuba.sk)

² Institute of Applied Mathematics, Faculty of Mathematics, Physics and Informatics, Comenius University, 842 48 Bratislava, Slovak Republic
(e-mail: sevcovic@fmph.uniba.sk)

Received: 1 October 2002 / Accepted: 15 April 2003
Published online: 24 February 2004 – © Springer-Verlag 2004

Communicated by: J. Kačur

Abstract. We propose a direct method for solving the evolution of plane curves satisfying the geometric equation $v = \beta(x, k, \nu)$ where v is the normal velocity, k and ν are the curvature and tangential angle of a plane curve $\Gamma \subset \mathbb{R}^2$ at a point $x \in \Gamma$. We derive and analyze the governing system of partial differential equations for the curvature, tangential angle, local length and position vector of an evolving family of plane curves. The governing equations include a nontrivial tangential velocity functional yielding uniform redistribution of grid points along the evolving family of curves preventing thus numerically computed solutions from forming various instabilities. We also propose a full space-time discretization of the governing system of equations and study its experimental order of convergence. Several computational examples of evolution of plane curves driven by curvature and external force as well as the geodesic curvatures driven evolution of curves on various complex surfaces are presented in this paper.

1 Introduction

In this paper we study evolution of a family of closed smooth plane curves $\Gamma_t : S^1 \rightarrow \mathbb{R}^2$, $t \geq 0$, driven by the normal velocity v which is assumed to be a function of the curvature k , tangential angle ν and position vector $x \in \Gamma_t$,

$$v = \beta(x, k, \nu). \quad (1)$$

Geometric equations of the form (1) can be often found in variety of applied problems like e.g. the material science, dynamics of phase boundaries in thermomechanics, in modeling of flame front propagation, in combustion, in computations of first arrival times of seismic waves, in computational

geometry, robotics, semiconductors industry, etc. They also have a special conceptual importance in image processing and computer vision. For an overview of important applications of (1) we refer to a book by Sethian [35].

Another interesting application of the geometric equation (1) arises from the differential geometry. The purpose is to investigate evolution of curves on a given surface driven by the geodesic mean curvature and prescribed external force. We restrict our attention to the case when the normal velocity \mathcal{V} is a linear function of the geodesic curvature \mathcal{K}_g and external force \mathcal{F} , i.e. $\mathcal{V} = \mathcal{K}_g + \mathcal{F}$ and the surface \mathcal{M} in \mathbb{R}^3 can be represented by a smooth graph. The idea how to analyze a flow of curves on a surface \mathcal{M} consists in vertical projection of surface curves into the plane. This allows for reducing the problem to the analysis of evolution of planar curves instead of surface ones. Although the geometric equation $\mathcal{V} = \mathcal{K}_g + \mathcal{F}$ is simple the description of the normal velocity v of the family of projected planar curves is rather involved. Nevertheless, it can be written in the form of equation (1). The precise form of the function β can be found in the next section.

Our methodology how to solve (1) is based on the so-called direct approach investigated by many authors (see e.g. [11–15, 24–29, 34]). The main idea is to represent the flow of planar curves by the position vector x which is a solution to the geometric equation $\partial_t x = \beta N + \alpha T$ where N , T are the unit inward normal and tangent vectors, resp. It turns out that one can construct a closed system of parabolic-ordinary differential equations for relevant geometric quantities: the curvature, tangential angle, local length and position vector. Other well-known techniques, like e.g. level-set method due to Osher and Sethian (cf. [35]) or phase-field approximations studied by Caginalp, Nochetto, Paolini, Verdi, Beneš (see e.g. [6, 7, 30]) treat the geometric equation (1) by means of a solution to a higher dimensional parabolic problem. In comparison to these methods, in the direct approach one space dimensional evolutionary problems are solved only.

Notice that the presence of a tangential velocity functional α in the position vector equation $\partial_t x = \beta N + \alpha T$ has no impact on the shape of evolving curves and therefore the most common setting $\alpha = 0$ has been chosen for analytical

* This work was supported by VEGA grants 1/0313/03 and 1/7677/20. The authors are also thankful to the Stefan Banach International Mathematical Center – Centre of Excellence, Institute of Mathematics PAN in Warsaw and ICM, Warsaw University, where a substantial part of the paper was finalized and numerical experiments were completed.

as well as numerical treatment by Abresch, Langer, Gage, Hamilton, Grayson, Angenent, Dziuk (see [1, 4, 12–15, 32]) and many others. Importance of a nontrivial tangential term has been emphasized and utilized in papers by Hou, Lowen-grub, Kimura, Deckelick, Mikula, Ševčovič in [11, 16, 17, 22, 26–28]. In [27, 28], the tangential velocity α has been determined in such a way that the initial redistribution of grid points is preserved along the evolution. In the case of isotropic and linear dependence of the flow on the curvature, the same redistribution strategy has been proposed by Hou *et al.* in [16, 17]. This approach significantly improved and stabilized all numerical computations obtained by the direct method. It has been documented by a variety of numerical experiments in [16, 17, 27, 28].

The governing system of PDEs are of convection – reaction – diffusion type. Our fully discrete numerical scheme is semi-implicit in time, i.e. all nonlinearities are treated from the previous time step and linear terms are discretized at the current time level. We solve tridiagonal systems in every time step in a fast and simple way. An undesirable, from a numerical point of view, behavior of strong reaction terms is overcome by an appropriate choice of a tangential redistribution functional. The method also allows us to choose of larger time steps without loss of stability. Stabilization in the convective terms is obtained by taking a sufficiently fine curve representation.

The outline of the paper is as follows: in the next section we present three areas in which geometric equations of the form (1) occur. A special attention is put on the analysis of a flow of curves on a simple surface by means of their vertical projection to the plane. We also show important connection between the geodesic flow of surface curves and the edge detection problem arising from the image segmentation theory. In Sect. 3 we derive a governing system of PDEs describing the evolution of plane curves satisfying (1). The system consists of a coupled parabolic-ordinary differential equations for the curvature, tangential angle, local length and position vector. These equations however contain one free parameter – tangential velocity of points on an evolving curve. In Sect. 4 we focus our attention to the problem how to choose a suitable tangential velocity functional guaranteeing uniform or asymptotically uniform redistribution of grid point along the evolved curve. We analyze two different strategies how to choose tangential velocity functional – nonlocal and local one. Qualitative aspects of solutions like existence and their limiting behavior are investigated in Sect. 5. In Sect. 6 numerical schemes for full space time discretization of the governing system of equations are presented. Results of numerical approximation of the mean curvature and external force driven flow of plane curves, edge detection problem in the image segmentation as well as the flow of curves on various complex surfaces are presented in Sect. 7.

2 Motivation

Throughout the paper we will be mainly concerned with applications in which the normal velocity v may depend on the position vector x , the tangential angle ν and the dependence on the curvature k is linear, i.e. $v = \beta(x, k, \nu)$ where

$$\beta(x, k, \nu) = a(x, \nu)k + c(x, \nu) \quad (2)$$

and $a > 0$ and c are smooth functions depending on x and ν .

2.1 Interface dynamics

If a solid phase occupies a subset $\Omega_s(t) \subset \Omega$ and a liquid phase – a subset $\Omega_l(t) \subset \Omega$, $\Omega \subset \mathbb{R}^2$, at a time t , then the phase interface is the set $\Gamma_t = \partial\Omega_s(t) \cap \partial\Omega_l(t)$ which is assumed to be a closed smooth embedded curve. The sharp-interface description of the solidification process is then described by the Stefan problem with a surface tension

$$\begin{aligned} \rho c \partial_t U &= \lambda \Delta U && \text{in } \Omega_s(t) \text{ and } \Omega_l(t), \\ [\lambda \partial_n U]_s^l &= -Lv && \text{on } \Gamma_t, \end{aligned} \quad (3)$$

$$\frac{\delta e}{\sigma}(U - U^*) = -\delta_2(\nu)k + \delta_1(\nu)v \text{ on } \Gamma_t, \quad (4)$$

subject to initial and boundary conditions for the temperature field U and initial position of the interface Γ (see e.g. [6, 34]). The constants ρ , c , λ represent material characteristics (density, specific heat and thermal conductivity), L is the latent heat per unit volume, U^* is a melting point and v is normal velocity of the interface. Discontinuity in the heat flux on the interface Γ_t is described by the Stefan condition (3). The relationship (4) is referred to as the Gibbs–Thomson law on the interface Γ_t , where δe is difference in entropy per unit volume between liquid and solid phases, σ is a constant surface tension, δ_1 is a coefficient of attachment kinetics and dimensionless function δ_2 describes anisotropy of the interface. One can see that the Gibbs–Thomson condition can be viewed as a geometric equation having the form (2).

In the series of papers [4, 5], Angenent and Gurtin studied perfect conductors where the problem can be reduced to a single equation on the interface. Following their approach and assuming a constant kinetic coefficient one obtains the equation

$$v = \beta(x, k, \nu) \equiv \delta(\nu)k + F$$

describing the interface dynamics. It is often referred to as the *anisotropic curve shortening equation* with a constant driving force F (energy difference between bulk phases) and a given anisotropy function δ .

2.2 Geodesic curvature driven flow of curves on a surface

Let us consider a flow of curves on a two dimensional surface \mathcal{M} in \mathbb{R}^3 . The surface $\mathcal{M} = \{(x, \varphi(x)) \in \mathbb{R}^3, x \in \Omega\}$ is assumed to be represented by a graph of a smooth function $\varphi: \Omega \subset \mathbb{R}^2 \rightarrow \mathbb{R}$ defined in a domain $\Omega \subset \mathbb{R}^2$. We assume the simplest possible case in which the normal velocity \mathcal{V} of a curve \mathcal{G} on \mathcal{M} is a linear function of its geodesic curvature \mathcal{K}_g and external force,

$$\mathcal{V} = \mathcal{K}_g + \mathcal{F} \quad (5)$$

where \mathcal{F} is the normal component of a given external force \mathbf{G} , i.e. $\mathcal{F} = \mathbf{G} \cdot \mathcal{N}$ and \mathcal{N} is the unit normal vector to \mathcal{G} belonging to the tangent space $T_x(\mathcal{M})$.

Hereafter, we will frequently use the abbreviation (x, z) standing for a vector $(x_1, x_2, z) \in \mathbb{R}^3$ where $x = (x_1, x_2) \in \mathbb{R}^2$. Any smooth closed curve \mathcal{G} on the surface \mathcal{M} can be then represented by its vertical projection to Ω , i.e.

$$\mathcal{G} = \{(x, \varphi(x)) \in \mathbb{R}^3, x \in \Gamma\}$$

where Γ is a planar curve in $\Omega \subset \mathbb{R}^2$ (see Fig. 1).

Our next goal is to derive a geometric equation for evolution of the family of planar curves $\Gamma_t, t \geq 0$, provided that the flow $\mathcal{G}_t, t \geq 0$, of surface curves satisfies (5). To this end, we have to find how the normal velocity v of Γ_t depends on geometric quantities corresponding to Γ_t . Straightforward calculations enables us to conclude that the unit inward normal and tangent vectors $\mathcal{N}, \mathcal{T} \in T_x(\mathcal{M})$ to a surface curve $\mathcal{G} \subset \mathcal{M}$ relative to \mathcal{M} are given by

$$\mathcal{T} = \frac{(\mathbf{T}, \nabla\varphi.\mathbf{T})}{(1 + (\nabla\varphi.\mathbf{T})^2)^{\frac{1}{2}}},$$

$$\mathcal{N} = \frac{((1 + (\nabla\varphi.\mathbf{T})^2)\mathbf{N} - (\nabla\varphi.\mathbf{T})(\nabla\varphi.\mathbf{N})\mathbf{T}, \nabla\varphi.\mathbf{N})}{((1 + |\nabla\varphi|^2)(1 + (\nabla\varphi.\mathbf{T})^2))^{\frac{1}{2}}}.$$

For a curve $\mathcal{G} = \{(x, \varphi(x)) \in \mathbb{R}^3, x \in \Gamma\}$ on a surface $\mathcal{M} = \{(x_1, x_2, \varphi(x_1, x_2)) \in \mathbb{R}^3, (x_1, x_2) \in \Omega\}$ the geodesic curvature \mathcal{K}_g is given by

$$\begin{aligned} \mathcal{K}_g = & -\sqrt{EG - F^2} (x_1''x_2' - x_1'x_2'' - \Gamma_{11}^2x_1'^3 + \Gamma_{22}^1x_2'^3 \\ & - (2\Gamma_{12}^2 - \Gamma_{11}^1)x_1'^2x_2' + (2\Gamma_{12}^1 - \Gamma_{22}^2)x_1'x_2'^2) \end{aligned}$$

where E, G, F are coefficients of the first fundamental form and Γ_{ij}^k are Christoffel symbols of the second kind. Here $(.)'$ denotes the derivative with respect to the unit speed parameterization of a curve on a surface. Taking into account that the

surface \mathcal{M} is a graph of a smooth function φ we obtain, after some calculations, that

$$\mathcal{K}_g = \frac{(1 + |\nabla\varphi|^2)^{\frac{1}{2}}k + \frac{\mathbf{T}^T \nabla^2 \varphi \mathbf{T}}{(1 + |\nabla\varphi|^2)^{\frac{1}{2}}} \nabla\varphi.\mathbf{N}}{(1 + (\nabla\varphi.\mathbf{T})^2)^{\frac{3}{2}}} \quad (6)$$

where $k, \mathbf{T}, \mathbf{N}$ are the curvature, unit tangent and inward normal vector of a plane curve $\Gamma \subset \Omega$. The external vector field \mathbf{G} is assumed to be perpendicular to the plane \mathbb{R}^2 and it depends on the vertical coordinate $z = \varphi(x)$ only. As a typical example one can consider gravitational like external force

$$\mathbf{G}(x) = -(0, 0, \gamma).$$

where $\gamma = \gamma(z) = \gamma(\varphi(x))$ is a given scalar ‘‘gravity’’ functional. Taking the normal component of such an external force we obtain expression for the driving term $\mathcal{F} = \mathbf{G}.\mathcal{N}$ in the form

$$\mathcal{F} = -\frac{\gamma(\varphi(x))}{((1 + |\nabla\varphi|^2)(1 + (\nabla\varphi.\mathbf{T})^2))^{\frac{1}{2}}} \nabla\varphi.\mathbf{N}. \quad (7)$$

Now we are in a position to derive a geometric equation $v = \beta(x, k, v)$ having the form of (1) for the normal velocity v of Γ_t in such way that corresponding family of surface curves \mathcal{G}_t satisfies (5). For description of the evolution of the position vector $x = x(\cdot, t) \in \mathbb{R}^2$ of a planar curve Γ_t we consider the position vector equation

$$\partial_t x = \beta \mathbf{N} + \alpha \mathbf{T} \quad (8)$$

where β and α are normal and tangential velocities of Γ_t , resp. Since $\mathcal{G}_t = \{(x, \varphi(x)), x \in \Gamma_t\}$ the normal velocity \mathcal{V} of \mathcal{G}_t satisfies

$$\begin{aligned} \mathcal{V} &= \partial_t(x, \varphi(x)).\mathcal{N} = (\mathbf{N}, \nabla\varphi.\mathbf{N}).\beta \mathcal{N} \\ &= \left(\frac{1 + |\nabla\varphi|^2}{1 + (\nabla\varphi.\mathbf{T})^2} \right)^{\frac{1}{2}} \beta. \end{aligned}$$

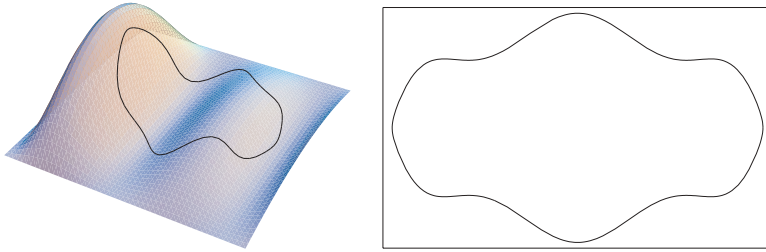


Fig. 1. A surface curve \mathcal{G} (left) and its projection Γ to the plane \mathbb{R}^2 (right)

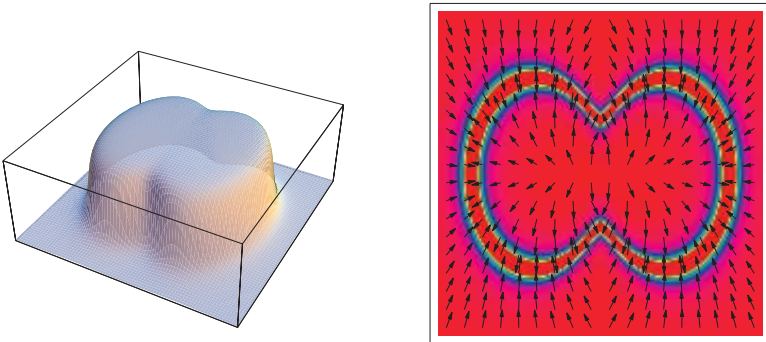


Fig. 2. An image intensity function $I(x)$ (left) corresponding to a ‘‘dumb-bell’’ image. The density plot of the function φ and corresponding vector field $-\nabla\varphi(x)$ (right)

It follows from (6) and (7) that the flow of surface curves $\mathcal{G}_t \subset \mathcal{M}$, $t \geq 0$, fulfills (5) if and only if the normal velocity v of the flow of planar curves Γ_t , $t \geq 0$, satisfies the geometric equation

$$v = \beta(x, k, \nu) \equiv a(x, \nu)k - b(x, \nu)\nabla\varphi(x) \cdot \mathbf{N} \quad (9)$$

where $a = a(x, \nu) > 0$ and $b = b(x, \nu)$ are smooth functions given by

$$a(x, \nu) = \frac{1}{1 + (\nabla\varphi \cdot \mathbf{T})^2}, \quad (10)$$

$$b(x, \nu) = \frac{1}{1 + |\nabla\varphi|^2} \left(\gamma(\varphi(x)) - \frac{\mathbf{T}^T \nabla^2 \varphi \mathbf{T}}{1 + (\nabla\varphi \cdot \mathbf{T})^2} \right).$$

Here $\varphi = \varphi(x)$ and $\mathbf{T} = (\cos \nu, \sin \nu)$, $\mathbf{N} = (-\sin \nu, \cos \nu)$. Notice that the function b is positive provided that $\gamma \gg 1$ is large enough. Furthermore, β is a 2π periodic function in ν variable and β is C^{k-2} smooth provided that $\varphi \in C^k$.

2.3 Image segmentation

A similar equation to (9) arises from the theory of image segmentation in which detection of object boundaries in the analyzed image plays an important rôle. A given B&W image can be represented by its intensity function $I : \mathbb{R}^2 \rightarrow [0, 255]$. The aim is to detect edges of the image, i.e. closed planar curves on which the gradient ∇I is large (see [18, 31]). The idea behind the so-called *active contour models* is to construct an evolving family of plane curves converging to an edge (see [19]). One can construct such a family respecting the geometric equation $v = \delta k + c$ where $c = c(x, \nu)$ is a driving force and $\delta = \delta(x, \nu) > 0$ is a smoothing coefficient. These functions may depend on the position vector x as well as orientation angle ν of a curve. If $c > 0$ then the driving force shrinks the curve whereas the impact of c is reversed in the case $c < 0$. Let us consider an auxiliary function $\varphi(x) = h(|\nabla I(x)|)$ where h is a smooth edge detector function like e.g. $h(s) = 1/(1+s^2)$. The gradient $-\nabla\varphi(x)$ has the important geometric property: it points towards regions where the norm of the gradient ∇I is large (see Fig. 2 right). Let us therefore take $c(x, \nu) = -b(\varphi(x))\nabla\varphi(x) \cdot \mathbf{N}$ and $\delta(x, \nu) = a(\varphi(x))$ where $a, b > 0$ are given smooth functions. Now, if an initial curve belongs to a neighborhood of an edge of the image and it is evolved according to the geometric equation

$$v = \beta(x, k, \nu) \equiv a(\varphi(x))k - b(\varphi(x))\nabla\varphi \cdot \mathbf{N}$$

then it is driven towards this edge. In the context of level set methods, edge detection techniques based on this idea were first discussed by Caselles et al. and Malladi et al. in [8, 23]. Later on, they have been revisited and improved in [9, 10, 20, 21].

3 Governing equations

In this section we derive a closed system of PDEs governing the evolution of a flow of plane curves satisfying geometric equation (1). An embedded regular plane curve Γ

can be parameterized by a smooth function $x : S^1 \rightarrow \mathbb{R}^2$, i.e. $\Gamma = \text{Image}(x) := \{x(u), u \in S^1\}$ and $g = |\partial_u x| > 0$. Taking into account the periodic boundary conditions at $u = 0, 1$ we can hereafter identify S^1 with the interval $[0, 1]$. The unit arc-length parameterization of a curve $\Gamma = \text{Image}(x)$ will be denoted by s . Then $ds = g du$. The tangent vector \mathbf{T} and the signed curvature k of Γ satisfy

$$\mathbf{T} = \partial_s x = g^{-1} \partial_u x,$$

$$k = \partial_s x \wedge \partial_s^2 x = g^{-3} \partial_u x \wedge \partial_u^2 x.$$

Moreover, we choose the unit inward normal vector \mathbf{N} such that $\mathbf{T} \wedge \mathbf{N} = 1$ where $\mathbf{a} \wedge \mathbf{b}$ is the determinant of the 2×2 matrix with column vectors \mathbf{a}, \mathbf{b} . By ν we denote the tangent angle to Γ , i.e. $\nu = \arg(\mathbf{T})$. Then $\mathbf{T} = (\cos \nu, \sin \nu)$ and, by Frenét's formulae, $\partial_s \mathbf{T} = k\mathbf{N}$, $\partial_s \mathbf{N} = -k\mathbf{T}$ and $\partial_s \nu = k$.

Let a regular smooth initial curve $\Gamma_0 = \text{Image}(x_0)$ be given. A family of plane curves $\Gamma_t = \text{Image}(x(\cdot, t))$, $t \in [0, T)$, satisfying (1) can be represented by a solution $x = x(u, t)$ to the position vector equation (8). Since this equation can not be solved without knowing k and ν we have to provide a closed system of governing equations for the curvature k , tangent angle ν , local length element $g = |\partial_u x|$ and the position vector x . The equations to follow are straightforward modifications of well-known geometric equations derived for the case of zero tangential velocity α (see e.g. [1, 2, 14]). In the general case when $\alpha \neq 0$ and $v = \beta(x, k, \nu)$ these equations were derived by the authors in [27] and [28]. Suppose that $\beta = \beta(x, k, \nu)$ is a smooth function, 2π periodic in the ν variable. According to [27] the equation for the tangential angle is: $\partial_t \nu = \partial_s \beta + \alpha k$. Since $\partial_s \nu = k$ and $\partial_s \beta = \beta'_k \partial_s k + \beta'_\nu \partial_s \nu + \nabla_x \beta \cdot \mathbf{T}$ we end up with the following closed system of parabolic-ordinary differential equations:

$$\partial_t k = \partial_s^2 \beta + \alpha \partial_s k + k^2 \beta, \quad (11)$$

$$\partial_t \nu = \beta'_k \partial_s^2 \nu + (\alpha + \beta'_\nu) \partial_s \nu + \nabla_x \beta \cdot \mathbf{T}, \quad (12)$$

$$\partial_t g = -gk\beta + \partial_u \alpha, \quad (13)$$

$$\partial_t x = \beta \mathbf{N} + \alpha \mathbf{T} \quad (14)$$

where $(u, t) \in [0, 1] \times (0, T)$, $ds = g du$, $\mathbf{T} = \partial_s x = (\cos \nu, \sin \nu)$, $\mathbf{N} = \mathbf{T}^\perp = (-\sin \nu, \cos \nu)$, $\beta = \beta(x, k, \nu)$. A solution (k, ν, g, x) to (11) – (14) is subject to initial conditions

$$k(\cdot, 0) = k_0, \quad \nu(\cdot, 0) = \nu_0, \quad g(\cdot, 0) = g_0, \quad x(\cdot, 0) = x_0(\cdot)$$

and periodic boundary conditions at $u = 0, 1$ except of ν for which we require the boundary condition $\nu(1, t) = \nu(0, t) + 2\pi$. The initial conditions for k_0, ν_0, g_0 and x_0 must satisfy natural compatibility constraints:

$$g_0 = |\partial_u x_0| > 0, \quad k_0 = g_0^{-3} \partial_u x_0 \wedge \partial_u^2 x_0, \quad \partial_u \nu_0 = g_0 k_0$$

following from (11) and Frenét's formulae applied to the initial curve $\Gamma_0 = \text{Image}(x_0)$.

Notice that the functional α is still undetermined and it may depend on variables k, ν, g, x in various ways including nonlocal dependence in particular. Suitable choices of the tangential velocity functional α are discussed in a more detail in the next section. Although α plays an important role in the governing equations resulting in dependence of k, ν, g, x on α , the family of planar curves $\Gamma_t = \text{Image}(x(\cdot, t))$, $t \in [0, T)$, is independent of a particular choice of α .

If we denote by L_t the length of a curve Γ_t , i.e. $L_t = \int_{\Gamma_t} ds = \int_0^1 g(u, t) du$, then by taking into account 1-periodicity of g and equation (13) we conclude

$$\frac{d}{dt}L_t + \langle k\beta \rangle_{\Gamma_t} L_t = 0 \quad (15)$$

where $\langle k\beta \rangle_{\Gamma}$ denotes the average of $k\beta$ over the curve Γ , i.e.

$$\langle k\beta \rangle_{\Gamma} = \frac{1}{L} \int_{\Gamma} k\beta ds.$$

4 The rôle of the tangential velocity functional

The main purpose of this section is to discuss various possible choices of the tangential velocity functional α appearing in the system of governing equations (11)–(14). In this system α can be viewed still as a free parameter which has to be determined in an appropriate way. Recall that k, v, g, x do depend on α but the family $\Gamma_t = \text{Image}(x(\cdot, t))$, $t \in [0, T)$, itself is independent of the particular choice of α .

To motivate further discussion, we recall some of computational examples in which the usual choice $\alpha = 0$ fails and may lead to serious numerical instabilities like e.g. formation of so-called swallow tails. In Figs. 3 and 4 we computed the mean curvature flow of two initial curves (bold faced curves). We chose $\alpha = 0$ in the experiment shown in Fig. 3. It should be obvious that numerically computed grid points merge in some parts of the curve Γ_t preventing thus numerical approximation of Γ_t , $t \in [0, T)$, to be continued beyond some time T which is still far away from the maximal time of existence T_{max} . These examples also showed that a suitable grid points redistribution governed by a nontrivial tangential velocity functional α is needed in order to compute the solution over its life-span.

The idea behind construction of a suitable tangential velocity functional α is rather simple and consists in the analysis of the quantity θ defined as follows:

$$\theta = \ln(g/L)$$

where $g = |\partial_u x|$ is a local length and L is a total length of a curve $\Gamma = \text{Image}(x)$. The quantity θ can be viewed as the logarithm of the relative local length g/L . Taking into account equations (13) and (15) we have

$$\partial_t \theta + k\beta - \langle k\beta \rangle_{\Gamma} = \partial_s \alpha. \quad (16)$$

By an appropriate choice of $\partial_s \alpha$ in the right hand side of (16) appropriately we can therefore control behavior of θ . Equation (16) can be also viewed as a kind of a constitutive relation determining redistribution of grid point along a curve.

4.1 Non-locally dependent tangential velocity functional

We first analyze the case when $\partial_s \alpha$ (and so does α) depends on other geometric quantities k, β and g in a nonlocal way. The simplest possible choice of $\partial_s \alpha$ is:

$$\partial_s \alpha = k\beta - \langle k\beta \rangle_{\Gamma} \quad (17)$$

yielding $\partial_t \theta = 0$ in (16). Consequently,

$$\frac{g(u, t)}{L_t} = \frac{g(u, 0)}{L_0} \quad \text{for any } u \in S^1, t \in [0, T_{max}).$$

Notice that α can be uniquely computed from (17) under the additional renormalization constraint: $\alpha(0, t) = 0$. In the sequel, tangential redistribution driven by a solution α to (17) will be referred to as a *parameterization preserving relative local length*. It has been first discovered and utilized by Hou et al. in [16, 17] and independently by the authors in [27, 28].

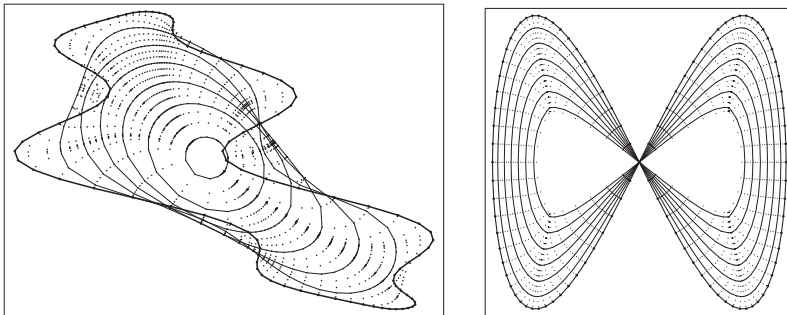


Fig. 3. Merging of numerically computed grid points in the case of zero tangential velocity functional α

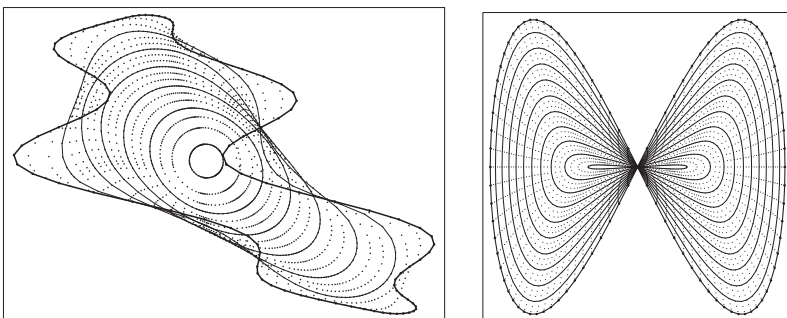


Fig. 4. Impact of a suitably chosen tangential velocity functional α on enhancement of the spatial grids redistribution

A general choice of α is based on the following setup:

$$\partial_s \alpha = k\beta - \langle k\beta \rangle_\Gamma + (e^{-\theta} - 1) \omega(t) \quad (18)$$

where $\omega \in L^1_{loc}([0, T_{max}))$. If we additionally suppose

$$\int_0^{T_{max}} \omega(\tau) d\tau = +\infty \quad (19)$$

then, after insertion of (18) into (16) and solving the ODE $\partial_t \theta = (e^{-\theta} - 1) \omega(t)$, we obtain $\theta(u, t) \rightarrow 0$ as $t \rightarrow T_{max}$ and hence

$$\frac{g(u, t)}{L_t} \rightarrow 1 \quad \text{as } t \rightarrow T_{max} \quad \text{uniformly w.r. to } u \in S^1.$$

In this case redistribution of grid points along a curve becomes uniform as t approaches the maximal time of existence T_{max} . We will refer to the parameterization based on (18) to as *an asymptotically uniform parameterization*. The impact of a tangential velocity functional defined as in (17) on enhancement of redistribution of grid points can be observed from two examples shown in Fig. 4 computed by the authors in [27].

Asymptotically uniform redistribution of grid points is of a particular interest in the case when the family $\{\Gamma_t, t \in [0, T)\}$ shrinks to a point as $t \rightarrow T_{max}$, i.e. $\lim_{t \rightarrow T_{max}} L_t = 0$. Then one can choose $\omega(t) = \kappa_2 \langle k\beta \rangle_{\Gamma_t}$ where $\kappa_2 > 0$ is a positive constant. By (15), $\int_0^t \omega(\tau) d\tau = -\kappa_2 \int_0^t \ln L_\tau d\tau = \kappa_2 (\ln L_0 - \ln L_t) \rightarrow +\infty$ as $t \rightarrow T_{max}$. On the other hand, if the length L_t is away from zero and $T_{max} = +\infty$ one can choose $\omega(t) = \kappa_1$, where $\kappa_1 > 0$ is a positive constant in order to meet the assumption (19).

Summarizing, in both types of grid points redistributions discussed above, a suitable choice of the tangential velocity functional α is given by a solution to

$$\partial_s \alpha = k\beta - \langle k\beta \rangle_\Gamma + (L/g - 1) \omega, \quad \alpha(0) = 0, \quad (20)$$

where $\omega = \kappa_1 + \kappa_2 \langle k\beta \rangle_\Gamma$ and $\kappa_1, \kappa_2 \geq 0$ are given constants.

If we insert tangential velocity functional α computed from (20) into (11)–(14) and make use of the identity $\alpha \partial_s k = \partial_s(\alpha k) - k \partial_s \alpha$ then the system of governing equations can be rewritten as follows:

$$\partial_t k = \partial_s^2 \beta + \partial_s(\alpha k) + k \langle k\beta \rangle_\Gamma + (1 - L/g) k \omega, \quad (21)$$

$$\partial_t v = \beta'_k \partial_s^2 v + (\alpha + \beta'_v) \partial_s v + \nabla_x \beta \cdot \mathbf{T}, \quad (22)$$

$$\partial_t g = -g \langle k\beta \rangle_\Gamma + (L - g) \omega, \quad (23)$$

$$\partial_t x = \beta \mathbf{N} + \alpha \mathbf{T}. \quad (24)$$

It is worth to note that the strong reaction term $k^2 \beta$ in (11) has been replaced by the averaged term $k \langle k\beta \rangle_\Gamma$ in (21). A similar phenomenon can be observed in (23). This is very important feature as it allows for construction of an efficient and stable numerical scheme discussed in Sect. 6.

4.2 Locally dependent tangential velocity functional

Another possibility for grid points redistribution along evolved curves is based on a tangential velocity functional defined

locally. If we take $\alpha = \partial_s \theta$, i.e. $\partial_s \alpha = \partial_s^2 \theta$ then the constitutive equation (16) reads as follows: $\partial_t \theta + k\beta - \langle k\beta \rangle_\Gamma = \partial_s^2 \theta$. Since this equation has a parabolic nature one can expect that θ will be redistributed along the curve Γ due to the diffusion process. The advantage of the particular choice

$$\alpha = \partial_s \theta = \partial_s \ln(g/L) = \partial_s \ln g \quad (25)$$

has been already observed by Deckelnick in [11]. He analyzed the mean curvature flow of planar curves (i.e. $v = k$) by means of a solution to the intrinsic heat equation

$$\partial_t x = \frac{\partial_u^2 x}{|\partial_u x|^2}, \quad u \in S^1, t \in (0, T),$$

describing evolution of the position vector x of a curve $\Gamma_t = \text{Image}(x(\cdot, t))$. By using Frenét's formulae we obtain $\partial_t x = k\mathbf{N} + \alpha\mathbf{T}$ where $\alpha = \partial_s \ln g = \partial_s \ln(g/L) = \partial_s \theta$.

Inserting the tangential velocity functional $\alpha = \partial_s \theta = \partial_s(\ln g)$ into (11)–(14) we obtain the following system of governing equations:

$$\partial_t k = \partial_s^2 \beta + \alpha \partial_s k + k^2 \beta, \quad (26)$$

$$\partial_t v = \beta'_k \partial_s^2 v + (\alpha + \beta'_v) \partial_s v + \nabla_x \beta \cdot \mathbf{T}, \quad (27)$$

$$\partial_t g = -gk\beta + g \partial_s^2(\ln g), \quad (28)$$

$$\partial_t x = \beta \mathbf{N} + \alpha \mathbf{T}. \quad (29)$$

Notice that equation (28) is a nonlinear parabolic equation whereas (23) is a nonlocal ODE for the local length g .

5 Qualitative behavior of solutions

5.1 Local existence, uniqueness and continuation of classical solutions

In this section we prove local in time existence of a classical solution of the governing system of equations (11)–(14) by means of the abstract theory of nonlinear analytic semigroups developed by Angenent in [3]. If we denote $\Phi = (k, \tilde{v}, g, x)$ where $\tilde{v}(u) = v(u) + 2\pi u$, $u \in S^1$, then the system of governing equations can be rewritten as a fully nonlinear PDE of the form

$$\partial_t \Phi = f(\Phi), \quad \Phi(0) = \Phi_0, \quad (30)$$

where $f(\Phi) = F(\Phi, \alpha(\Phi))$ and $F(\Phi, \alpha)$ is the right hand side of (21)–(24) if α is defined as in (20), or (26)–(29) if α is defined as in (25), resp. We had to shift the function v by $2\pi u$ because of the boundary condition $v(1) = v(0) + 2\pi$ imposed on the tangential angle v . Let $0 < \varrho < 1$ be fixed. By E_k^n, E_k^l we denote the following scale of Banach space

$$E_k^n = c^{2k+\varrho} \times c^{2k+\varrho} \times c^{1+\varrho} \times (c^{2k+\varrho})^2$$

$$E_k^l = c^{2k+\varrho} \times c^{2k+\varrho} \times c^{2k+\varrho} \times (c^{2k+\varrho})^2$$

where $k = 0, \frac{1}{2}, 1$, and $c^{2k+\varrho} = c^{2k+\varrho}(S^1)$ is the ‘‘little’’ Hölder space, i.e. the closure of $C^\infty(S^1)$ in the topology of the Hölder space $C^{2k+\varrho}(S^1)$ (see [2]). By the superscript ‘‘ n ’’ resp. ‘‘ l ’’ we distinguished the functional space setting for two different choices of the functional α discussed in Sects. 4.1 and 4.2,

resp. More precisely, depending on whether α is defined non-locally or locally, we define

$$\begin{aligned} E_k &= E_k^n & \text{if } \alpha \text{ is defined as in (20)} \\ E_k &= E_k^l & \text{if } \alpha \text{ is defined as in (25)} \end{aligned} \quad (31)$$

Let $\mathcal{O}_{\frac{1}{2}} \subset E_{\frac{1}{2}}$ be a bounded open subset such that $g > 0$ for any $(k, \tilde{v}, g, x) \in \mathcal{O}_{\frac{1}{2}}$. If the function $\beta : \mathbb{R}^2 \times \mathbb{R} \times \mathbb{R} \rightarrow \mathbb{R}$ is C^4 smooth and 2π periodic in the v variable then the mapping f is C^1 smooth from the open subset $\mathcal{O}_1 = \mathcal{O}_{\frac{1}{2}} \cap E_1 \subset E_1$ into E_0 .

If the Fréchet derivative $df(\bar{\Phi}) \in \mathcal{L}(E_1, E_0)$ belongs to the maximal regularity class $\mathcal{M}_1(E_0, E_1)$ for any $\bar{\Phi} \in \mathcal{O}_1$ where \mathcal{O}_1 is a neighborhood of the initial condition Φ_0 then, by [3, Theorem 2.7], the abstract equation (30) has a unique solution $\Phi \in Y^{(T)} = C([0, T], E_1) \cap C^1([0, T], E_0)$ on some small enough time interval $[0, T]$. According to [3] the class $\mathcal{M}_1(E_0, E_1) \subset \mathcal{L}(E_1, E_0)$ consists of those generators of analytic semigroups $A : D(A) = E_1 \subset E_0 \rightarrow E_0$ for which the linear equation $\partial_t \Phi = A\Phi + h(t)$, $t \in (0, 1]$, $\Phi(0) = \Phi_0$, has a unique solution $\Phi \in Y^{(1)}$ for any $h \in C([0, 1], E_0)$ and $\Phi_0 \in E_1$. In other words, (E_0, E_1) is the so-called *maximal parabolic regularity pair*.

Theorem 1. *Assume $\Phi_0 = (k_0, \tilde{v}_0, g_0, x_0) \in E_1$ where k_0 is the curvature, v_0 is the tangential vector, $g_0 = |\partial_u x_0| > 0$ is the local length element of an initial regular curve $\Gamma_0 = \text{Image}(x_0)$ and the Banach space E_k is defined as in (31). Assume $\beta = \beta(x, k, v)$ is a C^4 smooth and 2π -periodic function in the v variable such that $\min_{\Gamma_0} \beta'_k(x_0, k_0, v_0) > 0$ and α is defined either as in (20) or (25). Then there exists a unique solution $\Phi = (k, \tilde{v}, g, x) \in C([0, T], E_1) \cap C^1([0, T], E_0)$ of the governing system of equations (11)–(14) defined on some small time interval $[0, T]$, $T > 0$. Moreover, if Φ is the maximal solution defined on $[0, T_{max})$ then either $T_{max} = +\infty$ or $\liminf_{t \rightarrow T_{max}^-} \min_{\Gamma_t} \beta'_k(x, k, v) = 0$ or $T_{max} < +\infty$ and $\max_{\Gamma_t} |k| \rightarrow \infty$ as $t \rightarrow T_{max}$.*

Proof. Since $\partial_s v = k$ and $\partial_s \beta = \beta'_k \partial_s k + \beta'_v k + \nabla_x \beta \cdot \mathbf{T}$ where $\mathbf{T} = (\cos v, \sin v)$, $\mathbf{N} = (-\sin v, \cos v)$ the curvature equation (11) can be rewritten in the divergent form

$$\partial_t k = \partial_s(\beta'_k \partial_s k) + \partial_s(\beta'_v k) + \partial_s(\nabla_x \beta \cdot \mathbf{T}) + \alpha \partial_s k + k^2 \beta.$$

Moreover, as $k\mathbf{N} = \partial_s \mathbf{T} = \partial_s^2 x$ the last governing equation $\partial_t x = \beta \mathbf{N} + \alpha \mathbf{T}$ can be rewritten in the form

$$\partial_t x = a \partial_s^2 x + c \mathbf{N} + \alpha \mathbf{T}$$

where $c = c(x, k, v) \equiv \beta(x, k, v) - a(x, v)k$ and $a(x, v) = \beta'_k(x, k_0, v)$. There exists an open bounded subset $\mathcal{O}_{\frac{1}{2}} \subset E_{\frac{1}{2}}$ such that $\Phi_0 \in \mathcal{O}_1 = \mathcal{O}_{\frac{1}{2}} \cap E_1 \subset E_1$, $g > 0$, $\beta'_k(x, k, v) > 0$ and $a(x, v) > 0$ for any $(k, \tilde{v}, g, x) \in \mathcal{O}_1$. The linearisation of f at a point $\bar{\Phi} \in \mathcal{O}_1$ has the form: $A = df(\bar{\Phi}) \equiv \partial_u \bar{D} \partial_u + \bar{B} \partial_u + \bar{C}$ where $\bar{D} = \text{diag}(\bar{D}_{11}, \bar{D}_{22}, \bar{D}_{33}, \bar{D}_{44}, \bar{D}_{55})$, $\bar{D}_{ii} \in c^{1+e}$, $\bar{D}_{11} = \bar{D}_{22} = \bar{g}^{-2} \beta'_k(\bar{x}, \bar{k}, \bar{v})$, $\bar{D}_{44} = \bar{D}_{55} = \bar{a} \bar{g}^{-2} \in c^{1+e}$, $\bar{a} = a(\bar{x}, \bar{v})$. Furthermore, $\bar{B}_{ij}, \bar{C}_{ij} \in c^e$ for $i, j = 1, \dots, 5$. If α is defined as in (20) then $\bar{D}_{33} = 0$ and $\alpha \in C^1(\mathcal{O}_{\frac{1}{2}}, c^{2+e}(S^1))$. On the other hand, if α is defined as in (25) then $\bar{D}_{33} = \bar{g}^{-2}$ and $\alpha \in C^1(\mathcal{O}_{\frac{1}{2}}, c^e(S^1))$.

The linear operator A_1 defined by $A_1 \Phi = \partial_u(\bar{D} \partial_u \Phi)$, $D(A_1) = E_1 \subset E_0$ is a generator of an analytic semigroup on E_0 and, moreover, $A_1 \in \mathcal{M}_1(E_0, E_1)$ (see [3]). We can write $A = df(\bar{\Phi})$ as a sum $A_1 + A_2$ where $A_2 \in L(E_{\frac{1}{2}}, E_0)$. Thus $\|A_2 \Phi\|_{E_0} \leq C \|\Phi\|_{E_{\frac{1}{2}}} \leq C \|\Phi\|_{E_0}^{1/2} \|\Phi\|_{E_1}^{1/2}$ and so the linear operator A_2 is a relatively bounded linear perturbation of A_1 with zero relative bound (cf. [3]). With regard to [3, Lemma 2.5] the class \mathcal{M}_1 is closed with respect to such perturbations. Thus $df(\bar{\Phi}) \in \mathcal{M}_1(E_0, E_1)$ for any $\bar{\Phi} \in \mathcal{O}_1$. The proof of the short time existence of a solution Φ now follows from [3, Theorem 2.7].

It remains to prove that the maximal curvature becomes unbounded as $t \rightarrow T_{max}$ if $\liminf_{t \rightarrow T_{max}^-} \min_{\Gamma_t} \beta'_k > 0$ and $T_{max} < +\infty$. Suppose to the contrary that $\max_{\Gamma_t} |k| \leq M < \infty$ for any $t \in [0, T_{max})$. According to [2, Theorem 3.1] there exists a unique maximal solution $\Gamma : [0, T'_{max}) \rightarrow \Omega(\mathbb{R}^2)$ satisfying the geometric equation (1). Here $\Omega(\mathbb{R}^2)$ denotes the space of C^1 regular Jordan curves in the plane (cf. [2]). Moreover, Γ_t is a C^∞ smooth curve for any $t \in (0, T'_{max})$ and the maximum of the absolute value of the curvature tends to infinity as $t \rightarrow T'_{max}$. Thus $T_{max} < T'_{max}$ and therefore the curvature and subsequently \tilde{v} remain bounded in $C^{2+e'}$ norm on the interval $[0, T_{max}]$ for any $e' \in (e, 1)$. By the compactness argument the limit $\lim_{t \rightarrow T_{max}} \Phi(\cdot, t)$ exists and remains bounded in the space E_1 and one can continue the solution Φ beyond T_{max} , a contradiction.

Remark 1. In the general case where the normal velocity may depend on the position vector x , the maximal time of existence of a solution can be either finite or infinite. Indeed, as an example one can consider the unit ball $B = \{|x| < 1\}$ and function $\delta(x) = (|x| - 1)^p$ for $x \notin B$, $p > 0$. Suppose that $\Gamma_0 = \{|x| = R_0\}$ is a circle with a radius $R_0 > 1$ and the family Γ_t , $t \in [0, T)$, evolves according to the normal velocity function $\beta(x, k) = \delta(x)k$. Then, it is an easy calculus to verify that the family Γ_t approaches the boundary $\partial B = \{|x| = 1\}$ in a finite time $T_{max} < \infty$ provided that $0 < p < 1$ whereas $T_{max} = +\infty$ in the case $p = 1$.

5.2 First integrals and conserved quantities

Equation (15) from Sect. 3 is the first integral for the total length L_t of a curve Γ_t satisfying $v = \beta(x, k, v)$. This equality is rather general and is valid for any choice of the normal velocity β . Throughout this section we restrict our attention to the particular case when β is given by (9). It means that we are interested in the case when the corresponding family of surface curves evolves according to equation (5).

If Γ_t is parameterized by $x(\cdot, t) : S^1 \rightarrow \mathbb{R}^2$ then the length $\mathcal{L}_t = \text{Length}(\mathcal{G}_t)$ of its vertical projection \mathcal{G}_t to the surface $\mathcal{M} = \{(x, \varphi(x), x \in \mathbb{R}^2)\}$ is given by the value $\mathcal{J}(x(\cdot, t))$ of the total length functional

$$\mathcal{J}(x) = \int_{\mathcal{G}} dS = \int_{\Gamma} (1 + (\nabla \varphi \cdot \mathbf{T})^2)^{\frac{1}{2}} ds$$

where $dS = (1 + (\nabla \varphi \cdot \mathbf{T})^2)^{\frac{1}{2}} ds$. Calculating the Fréchet differential of \mathcal{J} we obtain

$$\mathcal{J}'(x)(y) = - \int_{\Gamma} (1 + |\nabla\varphi|^2)^{\frac{1}{2}} \mathcal{K}_g(y \cdot \mathbf{N}) ds.$$

Since $\mathcal{L}_t = \mathcal{J}(x(\cdot, t))$ we have

$$\begin{aligned} \frac{d}{dt} \mathcal{L}_t &= \mathcal{J}'(x(\cdot, t)) \partial_t x(\cdot, t) = - \int_{\Gamma_t} (1 + |\nabla\varphi|^2)^{\frac{1}{2}} \mathcal{K}_g \beta ds \\ &= - \int_{\Gamma_t} (1 + (\nabla\varphi \cdot \mathbf{T})^2)^{\frac{1}{2}} \mathcal{K}_g \mathcal{V} ds \\ &= - \int_{\mathcal{G}_t} \mathcal{K}_g \mathcal{V} dS. \end{aligned} \quad (32)$$

The flow of surface curves $\{\mathcal{G}_t, t \in [0, T]\}$ is length shortening provided that $\mathcal{V} = \mathcal{K}_g$, i.e. there is no external force \mathcal{F} in the geometric equation (5). The aim of the next proposition is to generalize (32) for the case of a nontrivial external force \mathcal{F} .

Proposition 1. *Let $\mathcal{H} : \mathbb{R} \rightarrow \mathbb{R}$ be a solution to the ODE: $\mathcal{H}'(z) = \gamma(z)\mathcal{H}(z)$, $z \in \mathbb{R}$. If the family $\mathcal{G}_t, t \in [0, T)$, of surface curves evolves according to the normal velocity $\mathcal{V} = \mathcal{K}_g + \mathcal{F}$ where $\mathcal{F} = \mathbf{G} \cdot \mathcal{N}$ and $\mathbf{G} = -(0, 0, \gamma(z))$, then*

$$\frac{d}{dt} \int_{\mathcal{G}_t} \mathcal{H}(z) dS = - \int_{\mathcal{G}_t} \mathcal{V}^2 \mathcal{H}(z) dS.$$

The proof of the above proposition can be found in the forthcoming paper [29]. As an immediate consequence we can conclude that the quantity $\int_{\mathcal{G}} \mathcal{H}(z) dS$ is a Lyapunov-like functional nonincreasing along trajectories of solutions to (5). Hence we exclude the existence of time periodic families or heteroclinic cycles of plane curves with normal velocity satisfying (5).

Corollary 1. *There exists no nontrivial time periodic family of surface curves $\{\mathcal{G}_t, t \geq 0\}$, with the normal velocity \mathcal{V} satisfying the geometric equation $\mathcal{V} = \mathcal{K}_g + \mathcal{F}$ where $\mathcal{F} = \mathbf{G} \cdot \mathcal{N}$ and $\mathbf{G} = -(0, 0, \gamma(z))$.*

6 Numerical schemes for full space-time discretization

In this section we will describe full space-time discretization scheme. We consider the normal velocity

$$v = \beta(x, k, v) \equiv a(x, v)k + c(x, v)$$

where

$$c(x, v) = -b(x, v)\nabla\varphi(x) \cdot \mathbf{N}$$

and the tangential velocity functional given by a linear combination of non-local and local tangential redistributions discussed in Sects. 4.1 and 4.2. Let us denote $\eta = \ln g$. Then we have $\theta = \ln(g/L) = \eta - \ln L$, and, for the redistribution functional α , we obtain

$$\partial_s \alpha = \varepsilon_1(k\beta - \langle k\beta \rangle_{\Gamma}) + \omega(L/g - 1) + \varepsilon_2 \partial_s^2 \eta \quad (33)$$

where $\varepsilon_1, \omega, \varepsilon_2$ are weights for parameterization preserving relative local length, asymptotically uniform parameterization and locally diffusive parameterization, respectively. Recall that the parameter setting: $\varepsilon_1 = 1, \varepsilon_2 = 0, \omega = \kappa_1 + \kappa_2 \langle k\beta \rangle_{\Gamma}$ with $\kappa_1, \kappa_2 \geq 0$ is associated with the nonlocally dependent tangential velocity functional α discussed in Sect. 4.1 whereas the choice $\varepsilon_1 = 0, \varepsilon_2 = 1, \omega = 0$ corresponds to the locally defined α from Sect. 4.2. The governing system of equations (11)–(14) can be rewritten in the form suitable for numerical approximation:

$$\partial_t k = \partial_s^2 \beta + \partial_s(\alpha k) + k(k\beta - \partial_s \alpha), \quad (34)$$

$$\partial_t v = \beta'_k \partial_s^2 v + (\alpha + \beta'_v) \partial_s v + \nabla_x \beta \cdot \mathbf{T}, \quad (35)$$

$$\partial_t \eta = -k\beta + \partial_s \alpha, \quad g = \exp(\eta), \quad (36)$$

$$\partial_t x = a(x, v) \partial_s^2 x + \alpha \partial_s x + c(x, v) \quad (37)$$

where $c(x, v) = c(x, v) \cdot \mathbf{N} = c(x, v)(-\sin v, \cos v)$. By using Frenet's formulae one can easily verify that the last equation (37) is equivalent to (14) in the case of linear dependence β on the curvature k .

In our computational method a numerical solution to the system (33)–(37) is represented by discrete plane points x_i^j where the index $i = 0, \dots, n$, denotes space discretization and the index $j = 0, \dots, m$, denotes a discrete time stepping. The approximation of an evolving curve in j -th discrete time step is thus given by a polygon with vertices $x_i^j, i = 0, \dots, n$, for which the periodicity condition $x_0^j = x_n^j$ is required. If we take a uniform division of the time interval $[0, T]$ with a time step $\tau = \frac{T}{m}$ and a uniform division of the fixed parameterization interval $[0, 1]$ with a step $h = \frac{1}{n}$, a point x_i^j corresponds to $x(ih, j\tau)$. It is worthwhile noting that due to the intrinsic character of the governing equations a spatial discretization step h does not appear in the numerical scheme in the case $\omega = 0$.

To construct the approximation of an evolved curve we will derive systems of difference equations corresponding to (33)–(37) to be solved at every discrete time step. Difference equations will be given for discrete quantities $\alpha_i^j, \eta_i^j, r_i^j, k_i^j, v_i^j, x_i^j, i = 1, \dots, n, j = 1, \dots, m$, representing approximations of the unknowns $\alpha, \eta, gh, k, v, x$. The fully discrete quantities represent time stepping of time dependent functions $\alpha_i(t), \eta_i(t), r_i(t) = |x_i(t) - x_{i-1}(t)|, k_i(t), v_i(t), x_i(t)$ which will be also used in the sequel. The function $\alpha_i(t)$ represents tangential velocity of a flowing node $x_i(t)$. Functions $\eta_i(t), r_i(t), k_i(t), v_i(t)$ represent piecewise constant approximations of the corresponding quantities in a flowing-in-time linear segment, the so-called *flowing finite volume* $[x_{i-1}(t), x_i(t)]$. We will also use the corresponding flowing dual volumes defined as: $[\tilde{x}_{i-1}, \tilde{x}_i]$, where $\tilde{x}_i = \frac{x_{i-1} + x_i}{2}$.

Our algorithm is semi-implicit in time. It means that all non-linear terms in equations are treated from the previous time step whereas linear terms are solved at the current time level. Such a discretization leads to a solution of linear systems of equations at every discrete time level. At the j -th time step, $j = 1, \dots, m$, we first find discrete values of the tangential velocity functional α_i^j . Then the values of the redistribution parameter η_i^j are computed and subsequently utilised for updating discrete local lengths r_i^j . Using already computed local lengths, tridiagonal systems with periodic bound-

ary conditions are constructed and solved for discrete curvature k_i^j , tangent angle v_i^j and position vector x_i^j .

In order to construct a discretization of (33)–(36) we subsequently integrate equations over flowing finite volume $[x_{i-1}, x_i]$. Then, at any time t , for the tangential velocity functional α we have

$$\begin{aligned} \int_{x_{i-1}}^{x_i} \partial_s \alpha ds &= \int_{x_{i-1}}^{x_i} \varepsilon_1 (k\beta - \langle k\beta \rangle_\Gamma) ds \\ &+ \int_{x_{i-1}}^{x_i} \omega (L/g - 1) + \varepsilon_2 \partial_s^2 \eta ds \end{aligned}$$

and thus

$$\begin{aligned} \alpha_i - \alpha_{i-1} &= \varepsilon_1 (r_i k_i \beta(\tilde{x}_i, k_i, v_i) - r_i \langle k\beta \rangle_\Gamma) \\ &+ \omega (L/n - r_i) + \varepsilon_2 \left(\frac{\eta_{i+1} - \eta_i}{q_i} - \frac{\eta_i - \eta_{i-1}}{q_{i-1}} \right). \end{aligned}$$

By taking discrete time stepping in the previous relation we obtain the following expression for *discrete values of the tangential velocity functional* α_i^j

$$\begin{aligned} \alpha_i^j &= \alpha_{i-1}^j + \omega (M^{j-1} - r_i^{j-1}) \\ &+ \varepsilon_1 (r_i^{j-1} k_i^{j-1} \beta(\tilde{x}_i^{j-1}, k_i^{j-1}, v_i^{j-1}) - r_i^{j-1} B^{j-1}) \\ &+ \varepsilon_2 \left(\frac{\eta_{i+1}^{j-1} - \eta_i^{j-1}}{q_i^{j-1}} - \frac{\eta_i^{j-1} - \eta_{i-1}^{j-1}}{q_{i-1}^{j-1}} \right) \end{aligned}$$

where

$$q_i^j = \frac{r_i^j + r_{i+1}^j}{2}, \quad \tilde{x}_i^{j-1} = \frac{x_{i-1}^{j-1} + x_i^{j-1}}{2}, \quad i = 1, \dots, n,$$

$\alpha_0^j = 0$, i.e. the point x_0^j is moved in the normal direction, and

$$M^{j-1} = \frac{1}{n} L^{j-1}, \quad L^{j-1} = \sum_{l=1}^n r_l^{j-1},$$

$$B^{j-1} = \frac{1}{L^{j-1}} \sum_{l=1}^n r_l^{j-1} k_l^{j-1} \beta(\tilde{x}_l^{j-1}, k_l^{j-1}, v_l^{j-1})$$

and $\omega = \kappa_1 + \kappa_2 B^{j-1}$ with κ_1, κ_2 being redistribution parameters.

Concerning discretization of equation (36) we proceed along the following lines:

$$\begin{aligned} \int_{x_{i-1}}^{x_i} \partial_t \eta ds &= \int_{x_{i-1}}^{x_i} -k\beta + \varepsilon_1 (k\beta - \langle k\beta \rangle_\Gamma) ds \\ &+ \int_{x_{i-1}}^{x_i} \omega (L/g - 1) + \varepsilon_2 \partial_s^2 \eta ds, \\ r_i \frac{d\eta_i}{dt} &= (\varepsilon_1 - 1) r_i k_i \beta(\tilde{x}_i, k_i, v_i) - \varepsilon_1 r_i \langle k\beta \rangle_\Gamma \\ &+ \omega (L/n - r_i) + \varepsilon_2 [\partial_s \eta]_{x_{i-1}}^{x_i}. \end{aligned}$$

Replacing the time derivative by time difference, approximating $\partial_s \eta$ in nodal points, taking all linear terms at the new time level j and all the remaining terms from the previous time level $j-1$ we obtain

$$\begin{aligned} r_i^{j-1} \frac{\eta_i^j - \eta_i^{j-1}}{\tau} &= (\varepsilon_1 - 1) r_i^{j-1} k_i^{j-1} \beta(\tilde{x}_i^{j-1}, k_i^{j-1}, v_i^{j-1}) \\ &- \varepsilon_1 r_i^{j-1} B^{j-1} + \omega (M^{j-1} - r_i^{j-1}) \\ &+ \varepsilon_2 \left(\frac{\eta_{i+1}^j - \eta_i^j}{q_i^{j-1}} - \frac{\eta_i^j - \eta_{i-1}^j}{q_{i-1}^{j-1}} \right), \end{aligned}$$

for $i = 1, \dots, n$, $\eta_0^j = \eta_n^j$, $\eta_{n+1}^j = \eta_1^j$. Note that this is either an updating formula in the case $\varepsilon_2 = 0$ or a tridiagonal system (if $\varepsilon_2 \neq 0$) for *new values of redistribution parameter* η . Next we *update local lengths* by the rule:

$$r_i^j = \exp(\eta_i^j), \quad i = 1, \dots, n, \quad r_0^j = r_n^j, \quad r_{n+1}^j = r_1^j.$$

Subsequently, new local lengths are used for approximation of intrinsic derivatives in (34)–(37). First, we derive a discrete analogy of the curvature equation (34). We have

$$\begin{aligned} \int_{x_{i-1}}^{x_i} \partial_t k ds &= \int_{x_{i-1}}^{x_i} \partial_s^2 \beta(x, k, v) ds \\ &+ \int_{x_{i-1}}^{x_i} \partial_s (\alpha k) ds + \int_{x_{i-1}}^{x_i} k (k\beta - \partial_s \alpha) ds, \\ r_i \frac{dk_i}{dt} &= [\partial_s \beta(x, k, v)]_{x_{i-1}}^{x_i} + [\alpha k]_{x_{i-1}}^{x_i} \\ &+ r_i k_i (k_i \beta(\tilde{x}_i, k_i, v_i) - (\alpha_i - \alpha_{i-1})). \end{aligned}$$

Now, by replacing the time derivative by time difference, approximating k in nodal points by the average value of neighboring segments, taking all linear terms at the new time level j and taking all the remaining terms from the previous time level $j-1$ we obtain a *tridiagonal system* subject to periodic boundary conditions imposed on *new discrete values of curvature*:

$$a_i^j k_{i-1}^j + b_i^j k_i^j + c_i^j k_{i+1}^j = d_i^j, \quad i = 1, \dots, n,$$

$$k_0^j = k_n^j, \quad k_{n+1}^j = k_1^j,$$

where

$$\begin{aligned} a_i^j &= \frac{\alpha_{i-1}^j}{2} - \frac{a(\tilde{x}_{i-1}^{j-1}, v_{i-1}^{j-1})}{q_{i-1}^j}, \\ b_i^j &= r_i^j \left(\frac{1}{\tau} - k_i^{j-1} \beta(\tilde{x}_i^{j-1}, k_i^{j-1}, v_i^{j-1}) + \alpha_i^j - \alpha_{i-1}^j \right) \\ &- \frac{\alpha_i^j}{2} + \frac{\alpha_{i-1}^j}{2} + \frac{a(\tilde{x}_i^{j-1}, v_i^{j-1})}{q_{i-1}^j} + \frac{a(\tilde{x}_i^{j-1}, v_i^{j-1})}{q_i^j}, \\ c_i^j &= -\frac{\alpha_i^j}{2} - \frac{a(\tilde{x}_{i+1}^{j-1}, v_{i+1}^{j-1})}{q_i^j}, \end{aligned}$$

$$d_i^j = \frac{r_i^j}{\tau} k_i^{j-1} + \frac{c(\tilde{x}_{i+1}^{j-1}, v_{i+1}^{j-1}) - c(\tilde{x}_i^{j-1}, v_i^{j-1})}{q_i^j} - \frac{c(\tilde{x}_i^{j-1}, v_i^{j-1}) - c(\tilde{x}_{i-1}^{j-1}, v_{i-1}^{j-1})}{q_{i-1}^j}.$$

In the next step we solve the tangent angle equation (35) using the following approximation:

$$\begin{aligned} \int_{x_{i-1}}^{x_i} \partial_t v ds &= \beta'_k(\tilde{x}_i, k_i, v_i) \int_{x_{i-1}}^{x_i} \partial_s^2 v ds + \int_{x_{i-1}}^{x_i} \alpha \partial_s v ds \\ &+ \beta'_v(\tilde{x}_i, k_i, v_i) \int_{x_{i-1}}^{x_i} \partial_s v ds + \int_{x_{i-1}}^{x_i} \nabla_x \beta(\tilde{x}_i, v_i, k_i) \cdot \mathbf{T} ds, \\ r_i \frac{dv_i}{dt} &= a(\tilde{x}_i, v_i) [\partial_s v]_{x_{i-1}}^{x_i} + [\alpha v]_{x_{i-1}}^{x_i} \\ &- v_i \int_{x_{i-1}}^{x_i} \partial_s \alpha ds + \beta'_v(\tilde{x}_i, k_i, v_i) [v]_{x_{i-1}}^{x_i} \\ &+ r_i \nabla_x \beta(\tilde{x}_i, v_i, k_i) \cdot (\cos v_i, \sin v_i). \end{aligned}$$

Again, values of v in nodal points are approximated by the average of neighboring segments values, the time derivative is replaced by the time difference. By applying a semi-implicit approach we obtain

$$\begin{aligned} r_i^j \frac{v_i^j - v_i^{j-1}}{\tau} &= a(\tilde{x}_i^{j-1}, v_i^{j-1}) \left(\frac{v_{i+1}^j - v_i^j}{q_i^j} - \frac{v_i^j - v_{i-1}^j}{q_{i-1}^j} \right) \\ &+ \alpha_i^j \frac{v_{i+1}^j + v_i^j}{2} - \alpha_{i-1}^j \frac{v_i^j + v_{i-1}^j}{2} - v_i^j (\alpha_i^j - \alpha_{i-1}^j) \\ &+ \beta'_v(\tilde{x}_i^{j-1}, k_i^{j-1}, v_i^{j-1}) \left(\frac{v_{i+1}^j - v_{i-1}^j}{2} \right) \\ &+ r_i^{j-1} \nabla_x \beta(\tilde{x}_i^{j-1}, v_i^{j-1}, k_i^j) \cdot (\cos v_i^{j-1}, \sin v_i^{j-1}). \end{aligned}$$

Collecting the corresponding terms we again end up with a *tridiagonal system* with periodic boundary conditions for new values of the tangent angle

$$A_i^j v_{i-1}^j + B_i^j v_i^j + C_i^j v_{i+1}^j = D_i^j, \quad i = 1, \dots, n,$$

$$v_0^j = v_n^j - 2\pi, \quad v_{n+1}^j = v_1^j + 2\pi,$$

where

$$\begin{aligned} A_i^j &= \frac{\alpha_{i-1}^j + \beta'_v(\tilde{x}_i^{j-1}, k_i^j, v_i^{j-1})}{2} - \frac{a(\tilde{x}_i^{j-1}, v_i^{j-1})}{q_{i-1}^j}, \\ B_i^j &= \frac{r_i^j}{\tau} - (A_i^j + C_i^j), \\ C_i^j &= -\frac{\alpha_i^j + \beta'_v(\tilde{x}_i^{j-1}, k_i^j, v_i^{j-1})}{2} - \frac{a(\tilde{x}_i^{j-1}, v_i^{j-1})}{q_i^j}, \\ D_i^j &= \frac{r_i^j}{\tau} v_i^{j-1} \\ &+ r_i^{j-1} \nabla_x \beta(\tilde{x}_i^{j-1}, v_i^{j-1}, k_i^j) \cdot (\cos v_i^{j-1}, \sin v_i^{j-1}). \end{aligned}$$

In order to construct discretization for (37) we integrate it in the dual volume $[\tilde{x}_{i-1}, \tilde{x}_i]$. We obtain

$$\begin{aligned} \int_{\tilde{x}_i}^{\tilde{x}_{i+1}} \partial_t x ds &= \int_{\tilde{x}_i}^{\tilde{x}_{i+1}} a(x, v) \partial_s^2 x ds \\ &+ \int_{\tilde{x}_i}^{\tilde{x}_{i+1}} \alpha \partial_s x ds + \int_{\tilde{x}_i}^{\tilde{x}_{i+1}} c(x, v) ds \\ q_i \frac{dx_i}{dt} &= a\left(x_i, \frac{v_i + v_{i+1}}{2}\right) [\partial_s x]_{\tilde{x}_i}^{\tilde{x}_{i+1}} + \alpha_i (\tilde{x}_{i+1} - \tilde{x}_i) \\ &+ q_i c\left(x_i, \frac{v_i + v_{i+1}}{2}\right), \\ q_i \frac{dx_i}{dt} &= a\left(x_i, \frac{v_i + v_{i+1}}{2}\right) \left(\frac{x_{i+1} - x_i}{r_{i+1}} - \frac{x_i - x_{i-1}}{r_i} \right) \\ &+ \alpha_i (\tilde{x}_{i+1} - \tilde{x}_i) + q_i c\left(x_i, \frac{1}{2}(v_i + v_{i+1})\right). \end{aligned}$$

By replacing \tilde{x}_i with the average of grid points, time derivative by time difference and using a semi-implicit approach in nonlinear terms we end up with *two tridiagonal systems for updating the position vector*

$$\mathcal{A}_i^j x_{i-1}^j + \mathcal{B}_i^j x_i^j + \mathcal{C}_i^j x_{i+1}^j = \mathcal{D}_i^j, \quad i = 1, \dots, n,$$

$$x_0^j = x_n^j, \quad x_{n+1}^j = x_1^j,$$

where

$$\begin{aligned} \mathcal{A}_i^j &= -\frac{a(x_i, \frac{1}{2}(v_i + v_{i+1}))}{r_i^j} + \frac{\alpha_i^j}{2}, \\ \mathcal{B}_i^j &= \frac{q_i^j}{\tau} - (\mathcal{A}_i^j + \mathcal{C}_i^j), \\ \mathcal{C}_i^j &= -\frac{a(x_i, \frac{1}{2}(v_i + v_{i+1}))}{r_{i+1}^j} - \frac{\alpha_i^j}{2}, \\ \mathcal{D}_i^j &= \frac{q_i^j}{\tau} x_i^{j-1} + q_i^j c\left(x_i^{j-1}, \frac{1}{2}(v_i^j + v_{i+1}^j)\right). \end{aligned}$$

Given a discretized initial curve x_i^0 further initial quantities for the algorithm are computed as follows:

$$R_i = (R_{i_1}, R_{i_2}) = x_i^0 - x_{i-1}^0, \quad i = 1, \dots, n,$$

$$R_0 = R_n, \quad R_{n+1} = R_1,$$

$$r_i^0 = |R_i|, \quad i = 0, \dots, n+1,$$

$$\eta_i^0 = \exp(r_i^0), \quad i = 0, \dots, n+1,$$

$$k_i = \frac{1}{2r_i^0} \operatorname{sgn}(R_{i-1} \wedge R_{i+1}) \arccos\left(\frac{R_{i+1} \cdot R_{i-1}}{r_{i+1}^0 r_{i-1}^0}\right),$$

$$i = 1, \dots, n, \quad k_0^0 = k_n^0, \quad k_{n+1}^0 = k_1^0,$$

$$v_0^0 = \arccos(R_{i_1}/r_i^0) \quad \text{if } R_{i_2} \geq 0,$$

$$v_0^0 = 2\pi - \arccos(R_{i_1}/r_i) \quad \text{if } R_{i_2} < 0,$$

$$v_i^0 = v_{i-1}^0 + r_i^0 k_i^0, \quad i = 1, \dots, n+1.$$

7 Computational results

In this section we summarize results of various numerical experiments. In the first part we present examples of curve evolution driven by the curvature and prescribed external force discussed in Sect. 2.1. In the next part we show examples of a geodesic flows with known explicit solutions and a flow on a more complex surface. Finally, we present some numerical experiments focusing on edge detection problems. In all figures of this section initial curves are plotted with a bold face and the numerical solution is given by further solid lines with points representing the motion of selected grid points during the curve evolution.

7.1 Examples of a flow of planar curves driven by the curvature and prescribed external force

In Figs. 5–6 to follow we present numerical solutions computed by the numerical scheme described in the previous section for the case $v = \beta(k, v) \equiv \delta k + F$. As an initial curve for computation shown in Fig. 5 we chose: $x_1(u) = \cos(2\pi u)$, $x_2(u) = 2 \sin(2\pi u) - 1.99 \sin^3(2\pi u)$, $u \in [0, 1]$. In Fig. 6 we considered an initial curve:

$$x_1(u) = (1 - C \cos^2(2\pi u)) \cos(2\pi u)$$

$$x_2(u) = (1 - C \cos^2(2\pi u)) \sin(2\pi u),$$

$u \in [0, 1]$ with $C = 0.7$. In Fig. 5 we chose $\tau = 0.00001$, 400 discrete grid points and we plotted every 150th time step. For computations depicted in Fig. 6 we took $\tau = 0.00001$ and 400 (Fig. 6 left) resp. 800 (Fig. 6 right) grid points. In all presented experiments we have used the nonlocal tangential velocity functional α defined in Sect. 4.1 with the parameters $\kappa_1 = \kappa_2 = 10$.

Although the number of grid points for representation of a curve might appear to be large in some of the previous experiments, solving tridiagonal systems constructed in Sect. 6 in each time step is still a fast and simple procedure.

7.2 Examples of a geodesic flow with known explicit solutions and experimental order of convergence

In this section we consider a flow of curves on a given graph surface driven by (5). Then the flow of vertically projected planar curves is driven by the geometric equation (9) with coefficients $a(x, v)$, $b(x, v)$ defined as in (10).

In the first example we have tested accuracy of the computed numerical blow-up time for the family of shrinking curves with finite extinction time. Comparison of exact and numerical blow-up of a family of shrinking circles on a surface $\mathcal{M} = \{(x, \varphi(x)), x \in \Omega \subset \mathbb{R}^2\}$ for various φ and $\mathbf{G} = -(0, 0, \gamma)$ is presented in Table 1. In this example the time step was $\tau = 0.0001$ and we chose the circle with radius 0.5 centered at the origin as an initial curve.

In the example shown in Fig. 7 we present inner and outer evolution of circles belonging to a “hat-like” surface and converging towards a circular valley. We chose $\varphi(x) = (1 - |x|^2)^2$, $t \in (0, 0.0315)$ and there was a strong external force $\gamma = 100$. Profiles of the radius $r = r(t)$ for inner and outer evolution are presented in Fig. 8.

The next example having an explicit solution is the family of shrinking circles belonging to a transversal plane. The projection to the base plane is the family of shrinking ellipses. More precisely, we consider a surface \mathcal{M} as a graph of $\varphi(x_1, x_2) = kx_1$ where $k \in \mathbb{R}$ is a fixed parameter. Let $r(t)$, $t \geq 0$, be a solution to ODE $\dot{r} = -1/r$, $r(0) = r_0 > 0$. Then $r(t) = \sqrt{2(T-t)}$ where $T = r_0^2/2$ and the normal velocity v of a family of shrinking ellipses $\Gamma_t = \{x(u, t), u \in$

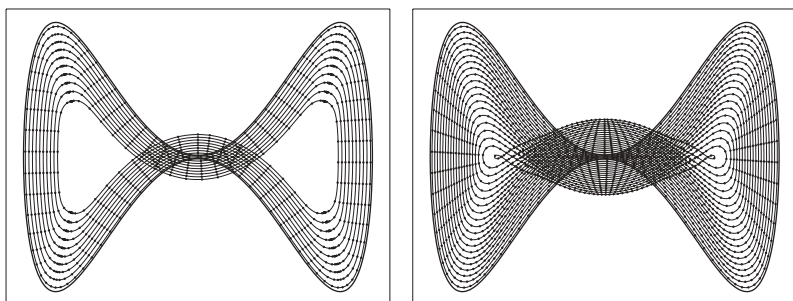


Fig. 5. Isotropic curvature driven motion, $\beta(k) = \delta k + F$, with $\delta = 1$, $F = 10$, without (left) and with (right) asymptotically uniform tangential redistribution of grid points. The merging of the grid points in the left figure is overcome by proper tangential redistribution in the right

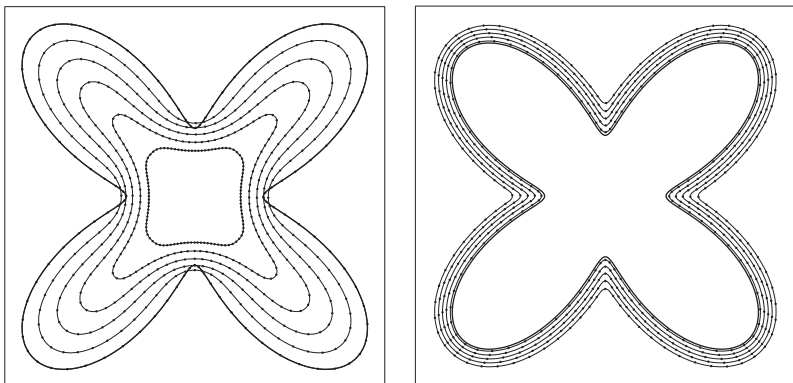


Fig. 6. Isotropic curvature driven motion of an initial non-convex curve including asymptotically uniform tangential redistribution of grid points; $\beta(k) = \delta k + F$, with $\delta = 1$ and $F = 10$ (left); $\delta = 0.1$ and $F = -10$ (right). Resolution of sharp corners in the case of a highly dominant forcing term $F = -10$ (right) is possible

Table 1. The exact T_{max} and numerical T_{max}^* blow-up times for the family of shrinking circles on a surface $\mathcal{M} = Graph(\varphi)$

$\varphi(x)$	γ	T_{max}	T_{max}^*
$1 - x ^2$	0	0.187489	0.1876
	1	0.269843	0.2700
$\sqrt{1 - x ^2}$	0	0.143833	0.1440
	1	0.169667	0.1698

$[0, 1]$, $x(u, t) = r(t) ((1 + k^2)^{-1/2} \cos(2\pi u), \sin(2\pi u))$ satisfies the geometric equation $v = \beta(x, k, v)$ where β is given by (9) with zero external force, i.e. $\gamma = 0$. Clearly, the family of shrinking circles $\mathcal{G}_t = \{(x, \varphi(x)), x \in \Gamma_t\}$ on the surface \mathcal{M} satisfies the geometric equation $\mathcal{V} = \mathcal{K}_g$. In the numerical experiment shown in Fig. 9 we chose $\varphi(x_1, x_2) = x_1$, $t \in (0, 0.5)$, $\gamma = 0$ and $r_0 = 1$.

An important tool for hard testing numerical algorithms is the so-called experimental order of convergence (EOC). The idea behind the definition of EOC is rather simple. Suppose that a numerical scheme has an order of convergence α with respect to a spatial discretization parameter h . Here h can be defined as: $h = 1/n$ where n is the number of grid points. It means that the error $err(h)$ (calculated in a certain prescribed norm) of an approximate numerical solution and the true solution satisfies $err(h) \approx h^\alpha$. Now if we halve the dis-

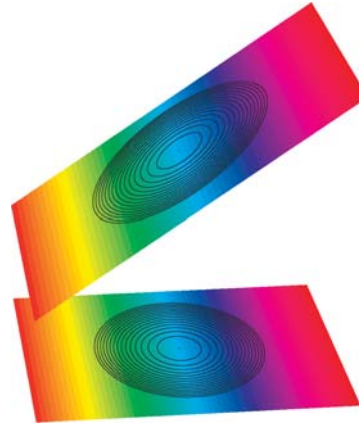


Fig. 9. A geodesic flow with no external force ($\gamma = 0$) on an affine plane and its vertical projection to the plane. We plot inner evolution of an initial ellipse corresponding to a circle with radius $r_0 = 1$ belonging to transversal plane over the time interval $(0, 0.5)$

cretization step h we can determine the exponent α of EOC as follows:

$$\alpha = \log_2 (err(h)/err(h/2)) .$$

We have tested the experimental order of convergence for the explicit example of shrinking circles on a transversal plane. Since the solved system of governing equations has the parabolic nature we adopted the natural constraint between time stepping and space discretization: $\tau = h^2/2$. In Table 2 we present results obtained by using nonlocal tangential velocity functional defined as in (20) whereas in Table 3 we summarize results obtained by using the locally depending tangential velocity functional defined as in (25). From the EOC point of view those two methods seem to have the same strength measured in terms of the EOC.

The last example of this section illustrates a geodesic flow $\mathcal{V} = \mathcal{K}_g$ on a surface with two sufficiently high humps. In Fig. 10 we considered a surface \mathcal{M} defined as a graph of the function $\varphi(x) = 6(f(x_1 - 1, x_2) + f(x_1 + 1, x_2))$ where $f(x) = 2^{-1/(1-|x|^2)}$ for $|x| < 1$ and $f(x) = 0$ for $|x| \geq 1$ is a smooth bump function. We took the time step $\tau = 0.0002$. Initial curve was an ellipse centered at the origin with axes 2 and $\sqrt{2}$. The spatial mesh contained 400 grid points. The initial curve was evolved until the time $T = 13$. As it can

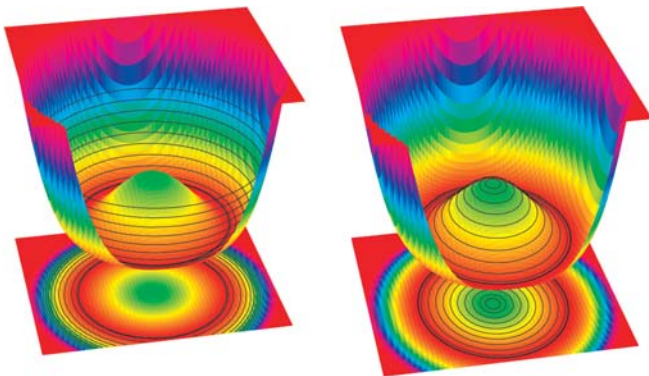


Fig. 7. A geodesic flow on the “hat-like” surface and its vertical projection to the plane. Outer and inner evolutions of initial circles T_0 with radii $r_0 = 1.5$ (left) and $r_0 = 0.1$ (right)

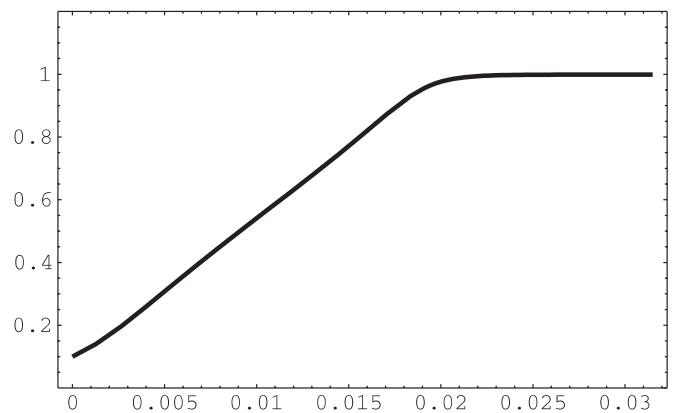
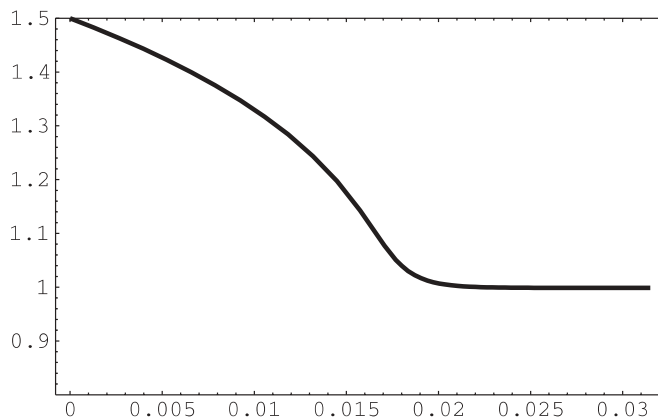


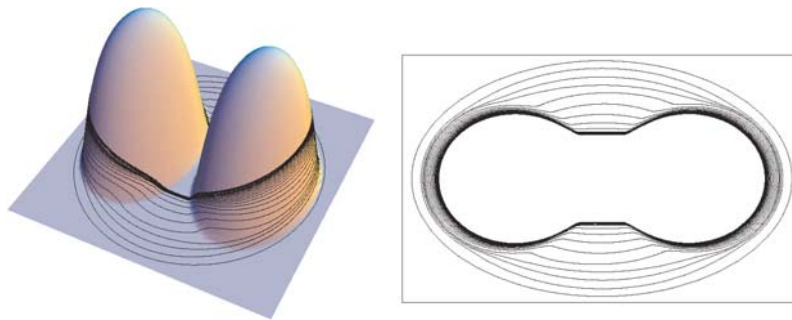
Fig. 8. Time evolution of the radius of shrinking circles (left) and expanding circles (right)

Table 2. Computation using the nonlocal tangential velocity α defined as in (20); $L^p((0, T), L^2(S^1))$ errors and their EOC for x, k, v and g

h	p	x	eoc	k	eoc	v	eoc	g	eoc
0.1	2	0.009398		0.07258		0.1286		0.03289	
	∞	0.01421		0.1162		0.1371		0.05433	
0.05	2	0.004015	1.227	0.03388	1.099	0.06842	0.9109	0.008914	1.884
	∞	0.005955	1.255	0.06471	0.8445	0.07381	0.8939	0.01483	1.873
0.025	2	0.001877	1.097	0.0165	1.038	0.03473	0.978	0.002296	1.957
	∞	0.002761	1.109	0.03347	0.9508	0.03761	0.9727	0.003808	1.961
0.0125	2	0.0009225	1.025	0.00827	0.9961	0.01743	0.9944	0.0005814	1.982
	∞	0.001352	1.031	0.01705	0.9734	0.01889	0.9931	0.0009625	1.984
0.00625	2	0.0004588	1.008	0.004105	1.011	0.008723	0.9991	0.0001454	1.999
	∞	0.0006711	1.01	0.008483	1.007	0.009458	0.9983	0.0002404	2.001

Table 3. Computation using the local tangential velocity α defined as in (25); $L^p((0, T), L^2(S^1))$ errors and their EOC for x, k, v and g

h	p	x	eoc	k	eoc	v	eoc	g	eoc
0.1	2	0.009608		0.07163		0.1286		0.03324	
	∞	0.01463		0.1135		0.1371		0.05545	
0.05	2	0.004064	1.241	0.03369	1.088	0.06845	0.9095	0.009231	1.849
	∞	0.006049	1.274	0.06387	0.83	0.07381	0.8939	0.01549	1.84
0.025	2	0.001889	1.106	0.01642	1.037	0.03475	0.9779	0.002389	1.95
	∞	0.00278	1.122	0.03318	0.9447	0.03761	0.9727	0.003985	1.958
0.0125	2	0.0009264	1.028	0.008235	0.9954	0.01744	0.9944	0.0006056	1.98
	∞	0.001356	1.035	0.01692	0.9719	0.01889	0.9931	0.001008	1.984
0.00625	2	0.0004604	1.009	0.004088	1.01	0.008728	0.999	0.0001515	1.999
	∞	0.0006729	1.011	0.00842	1.006	0.009458	0.9983	0.0002517	2.001


Fig. 10. A geodesic flow on a surface with two sufficiently high humps (left) and its vertical projection to the plane (right). The evolving family of surface curves approaches a closed geodesic as $t \rightarrow \infty$

be seen from Fig. 10 the evolving family of surface curves approaches a closed geodesic as $t \rightarrow \infty$. The existence of a closed geodesic curve follows from a simple calculation of the lower bound of the length of a curve passing through tops of both humps at the same moment which should be greater than $4\sqrt{3^2 + 1^2} \approx 12.64$. Since the length of the initial curve is approximately 10.81 and the flow of surface curves is length shortening (see Sect. 5.2) the family of surface curves converges to a nontrivial closed geodesic with the length strictly less than 10.81.

7.3 Edge detection examples

Finally, we apply our computational method to the image segmentation problem. First we treat the methodology for edge

detection discussed in Sect. 2.3. Let us consider the normal velocity $v = \beta(x, k, v)$ where

$$\beta(x, k, v) = \varphi(x)k - b(\varphi(x))\nabla\varphi(x).N,$$

$\varphi(x) = h(|\nabla I(x)|)$, $h(s) = \frac{1}{1+s^2}$ and $I(x)$ is a given image intensity function. The numerical experiment is shown in Fig. 11. We look for an edge in a 2D slice of a real 3D echocardiography which was prefiltered by the method of [33]. The testing data set (the image function I) is a courtesy of Prof. Claudio Lamberti, DEIS, University of Bologna. We have inserted an initial ellipse into the slice close to an expected edge (Fig. 11 left). Then it was evolved according to the normal velocity described above using the time stepping $\tau = 0.0001$ and nonlocal redistribution strategy from Sect. 4.1 with parameters $\kappa_1 = 20$, $\kappa_2 = 1$ until the limiting curve has

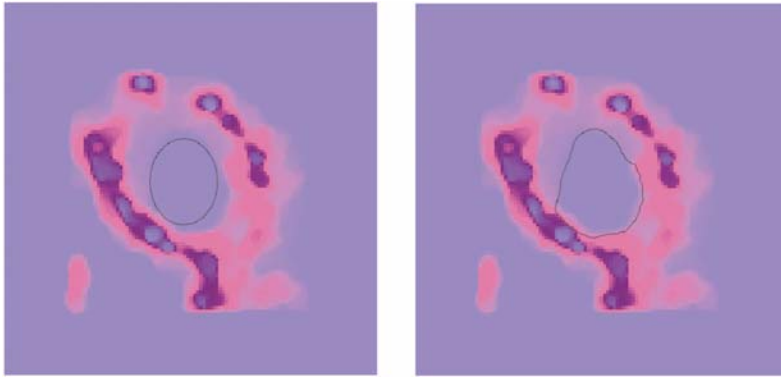


Fig. 11. An initial ellipse is inserted into the 2D slice of a prefiltered 3D echocardiography (*left*), the slice together with the limiting curve representing the edge (*right*)

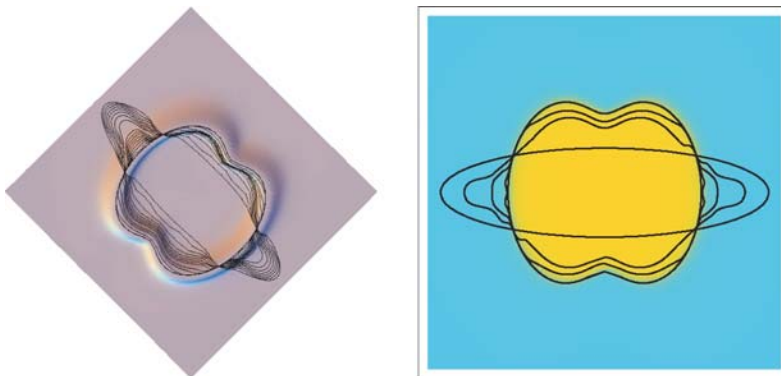


Fig. 12. A geodesic flow on a flat surface with a sharp narrow valley (*left*) and its vertical projection to the plane with density plot of the image intensity function $I(x)$ (*right*)

been formed (400 time steps). The final curve representing the edge in the slice can be seen in Fig. 11 right.

Next we present results for the image segmentation problem computed by means of a geodesic flow with external force discussed in Sect. 2.2. We consider an artificial image whose intensity function

$$I(x) = \frac{1}{2} + \frac{1}{\pi} \operatorname{arctg} \left(12.5 - 100 \left(|x| \frac{2x_1^2 + |x|^2}{4x_1^2 + |x|^2} \right)^2 \right)$$

is depicted in Fig. 2. If we take $\varphi(x) = 1/(1 + |\nabla I(x)|^2)$ then the surface \mathcal{M} defined as a graph of φ has a sharp narrow valley corresponding to points of the image in which the gradient $|\nabla I(x)|$ is very large representing thus an edge in the image. In contrast to the previous example shown in Fig. 11 we will make use of the flow of curves on a surface \mathcal{M} driven by the geodesic curvature and strong “gravitational-like” external force \mathcal{F} . According to Sect. 2.2 such a surface flow can be represented by a family of vertically projected plane curves driven by the normal velocity

$$v = a(x, v)k - b(x, v)\nabla\varphi(x) \cdot N$$

where coefficients a, b are defined as in (10) with strong external force coefficient $\gamma = 100$. Results of computation are presented in Fig. 12.

8 Discussion

In this paper we investigated evolution of plane curves driven by the curvature and external force. We have also analyzed

a flow of curves on simple surfaces driven by the geodesic curvature and external force. We showed how to reduce the flow of curves on a surface to a flow of vertically projected curves in the plane. The geometric equation for the corresponding flow of plane curves involves the curvature, anisotropy as well as the position vector. This makes the analysis of the governing equations considerably harder. We derived and analyzed a closed system of PDEs for all relevant geometric quantities. We constructed an efficient numerical scheme for solving the governing system of equations and study its experimental order of convergence. Impact of a nontrivial tangential velocity functional on numerically computed solution has been also analyzed. We presented various examples illustrating capability of the direct approach for solving curvature driven flow of plane and/or surface curves.

References

1. Abresch, U., Langer, J.: The normalized curve shortening flow and homothetic solutions. *J. Diff. Geom.* 23, 175–196 (1986)
2. Angenent, S.B.: Parabolic equations for curves on surfaces I: Curves with p-integrable curvature. *Annals of Mathematics* 132, 451–483 (1990)
3. Angenent, S.B.: Nonlinear analytic semiflows. *Proc. R. Soc. Edinb., Sect. A* 115, 91–107, (1990)
4. Angenent, S.B., Gurtin, M.E.: Multiphase thermomechanics with an interfacial structure 2. Evolution of an isothermal interface. *Arch. Rat. Mech. Anal.* 108, 323–391 (1989)
5. Angenent, S.B., Gurtin, M.E.: General contact angle conditions with and without kinetics. *Quarterly of Appl. Math.* 54(3), 557–569 (1996)
6. Beneš, M.: Mathematical and computational aspects of solidification of pure crystalline materials. *Acta Math. Univ. Comenianae* 70, 123–151 (2001)

7. Caginalp, G.: The dynamics of a conserved phase field system: Stefan-like, Hele-Shaw, and Cahn-Hilliard models as asymptotic limits. *IMA J. Appl. Math.* 44, 77–94 (1990)
8. Caselles, V., Catté, F., Coll, T., Dibos, F.: A geometric model for active contours in image processing. *Numerische Mathematik* 66, 1–31 (1993)
9. Caselles, V., Kimmel, R., Sapiro, G.: Geodesic active contours. *International Journal of Computer Vision* 22, 61–79 (1997)
10. Caselles, V., Kimmel, R., Sapiro, G., Sbert, C.: Minimal surfaces: a geometric three dimensional segmentation approach. *Numerische Mathematik* 77, 423–451 (1997)
11. Deckelnick, K.: Weak solutions of the curve shortening flow. *Calc. Var. Partial Differ. Equ.* 5, 489–510 (1997)
12. Dziuk, G.: Convergence of a semi discrete scheme for the curve shortening flow. *Math. Models Methods Appl. Sci.* 4, 589–606 (1994)
13. Dziuk, G.: Discrete anisotropic curve shortening flow. *SIAM J. Numer. Anal.* 36, 1808–1830 (1999)
14. Gage, M., Hamilton, R.S.: The heat equation shrinking convex plane curves. *J. Diff. Geom.* 23, 69–96 (1986)
15. Grayson, M.: The heat equation shrinks embedded plane curves to round points. *J. Diff. Geom.* 26, 285–314 (1987)
16. Hou, T.Y., Lowengrub, J., Shelley, M.: Removing the stiffness from interfacial flows and surface tension. *J. Comput. Phys.* 114, 312–338 (1994)
17. Hou, T.Y., Klapper, I., Si, H.: Removing the stiffness of curvature in computing 3-d filaments. *J. Comput. Phys.* 143, 628–664 (1998)
18. Kačur, J., Mikula, K.: Solution of nonlinear diffusion appearing in image smoothing and edge detection. *Applied Numerical Mathematics* 17, 47–59 (1995)
19. Kass, M., Witkin, A., Terzopoulos, D.: Snakes: active contour models. *International Journal of Computer Vision* 1, 321–331 (1987)
20. Kichenassamy, S., Kumar, A., Olver, P., Tannenbaum, A., Yezzi, A.: Gradient flows and geometric active contours models, in *Proceedings International Conference on Computer Vision'95*, Boston, 1995
21. Kichenassamy, S., Kumar, A., Olver, P., Tannenbaum, A., Yezzi, A.: Conformal curvature flows: from phase transitions to active vision. *Arch. Rational Mech. Anal.* 134, 275–301 (1996)
22. Kimura, M.: Numerical analysis for moving boundary problems using the boundary tracking method. *Japan J. Indust. Appl. Math.* 14, 373–398 (1997)
23. Malladi, R., Sethian, J., Vemuri, B.: Shape modeling with front propagation: a level set approach. *IEEE Trans. Pattern Anal. Machine Intelligence* 17, 158–174 (1995)
24. Mikula, K., Kačur, J.: Evolution of convex plane curves describing anisotropic motions of phase interfaces. *SIAM J. Sci. Comput.* 17, 1302–1327 (1996)
25. Mikula, K.: Solution of nonlinear curvature driven evolution of plane convex curves. *Appl. Numer. Math.* 21, 1–14 (1997)
26. Mikula, K., Ševčovič, D.: Solution of nonlinearly curvature driven evolution of plane curves. *Appl. Numer. Math.* 31, 191–207 (1999)
27. Mikula, K., Ševčovič, D.: Evolution of plane curves driven by a nonlinear function of curvature and anisotropy. *SIAM J. Appl. Math.* 61, 1473–1501 (2001)
28. Mikula, K., Ševčovič, D.: A direct method for solving an anisotropic mean curvature flow of plane curves with an external force. submitted
29. Mikula, K., Ševčovič, D.: Evolution of curves on a surface driven by the geodesic curvature and external force. submitted
30. Nochetto, R., Paolini, M., Verdi, C.: Sharp error analysis for curvature dependent evolving fronts. *Math. Models Methods Appl. Sci.* 3, 711–723 (1993)
31. Perona, P., Malik, J.: Scale space and edge detection using anisotropic diffusion. *Proc. IEEE Computer Society Workshop on Computer Vision* 1987
32. Sapiro, G., Tannenbaum, A.: On affine plane curve evolution. *J. Funct. Anal.* 119, 79–120 (1994)
33. Sarti, A., Mikula, K., Sgallari, F.: Nonlinear multiscale analysis of three-dimensional echocardiographic sequences. *IEEE Trans. on Medical Imaging* 18, 453–466 (1999)
34. Schmidt, A.: Computation of three dimensional dendrites with finite elements. *J. Comput. Phys.* 125, 293–312 (1996)
35. Sethian, J.A.: *Level Set Methods and Fast Marching Methods: Evolving Interfaces in Computational Geometry, Fluid Mechanics, Computer Vision, and Material Science*. New York: Cambridge University Press 1999